

# A Novel Bi-Directional Isolated Power Flow Dc–Dc Converter for Hybrid System

R. Karthikeyan<sup>1</sup>, A.Santhosh kumar<sup>2</sup> and D.Deenadayalan<sup>3</sup>

**Abstract**—In Electrical power systems in future uninterruptible power supplies or electrical vehicles may employ hybrid energy sources, such as fuel cells and super capacitors. It will be necessary to efficiently draw the energy from these two sources as well as recharge the energy storage elements by the dc bus. In this paper, a bidirectional isolated dc–dc converter controlled by phase-shift angle and duty cycle for the fuel-cell hybrid energy system is analyzed and designed. The proposed topology minimizes the number of switches and their associated gate driver components by using two high-frequency transformers that combine a half-bridge circuit and a full-bridge circuit together on the primary side. The voltage doubler circuit is employed on the secondary side. The current-fed input can limit the input current ripple that is favorable for fuel cells. This paper describes the operation principle of the proposed converter, the ZVS conditions, and the quasi-optimal design in depth. The fuel input voltage is given to the boost converter, where it is stepped up the voltage fed to the coupled transformer and one more half bridge construct connected with series with dc load to obtain 600-V tested to verify the effectiveness of the presented converter can be simulated by using MATLAB/SIMULINK. It can be used for high power applications.

**Index Term** — Bidirectional dc–dc converter, current-fed, fuel cell (FC), phase shift, super capacitor (SC).

## 1 Introduction

Renewable energy is becoming increasingly important and prevalent in distribution systems, which provide different choices to electricity consumers whether they receive power from the main electricity source. Hybrid renewable energy systems are becoming popular for remote area power generation applications due to advances in renewable energy technologies and subsequent rise in prices of petroleum products. A hybrid energy system usually consists of two or more renewable energy sources used together to provide increased system efficiency as well as greater balance in energy supply. The system should be enough flexible to adapt to the existing power generators, as well as changing habits of users when power supply is available continuously, sufficiently reliable for use in remote areas. The hybrid system based on fuel cells (FCs) and super capacitors (SCs) as an environmentally renewable energy system has been applied in many fields, such as hybrid electric vehicle, uninterruptible power supply (UPS), and so on. Compared to diesel generators and batteries, FCs are electrochemical devices that convert the chemical potential of the hydrogen into electric power directly with consequent high conversion efficiency, so it has the possibility to obtain the extended runtime range with the combustible feed from the outside. But one of the main weak points of the FC is its slow dynamics because of the limited speed of hydrogen delivery system and the chemical reaction in the membranes with a slow time constant. Hence, during the warming-up stage or load transient, SCs are utilized as the auxiliary power source for smoothing the output power. In addition, the fuel-cell

output voltage is varied widely, almost 2:1, depending on the load condition, and the terminal voltage of the SC bank is also variable during charging and discharging periods. Thus, it is very important for the conversion system to be capable of harvesting power from these two different power sources efficiently in widely input voltage range and load conditions.

In recent years, many configurations of a hybrid dc power conversion system relating to FCs and SCs have been proposed. Connecting FCs and SCs by two individual dc–dc converters separately to a mutual dc voltage bus is the most common configuration which offers many advantages, especially, faster and more stable system response. However, it increases the system cost and power losses. A multiple dc voltage bus, which connects FCs and SCs to different cascaded voltage buses through converters, is also a widely used configuration [1], [11] but the disadvantages are high power losses and low reliability.

## 2 Basic Operation Principles of the Hybrid Bidirectional Dc–Dc Converter

The bidirectional dc-dc converter in fig.1 has become a promising option for many power related systems, including hybrid vehicle, fuel cell vehicle, renewable energy system and so forth. It not only reduces the cost and improves efficiency, but also improves the performance of the system. Most of the existing bidirectional dc-dc converters fall into the generic circuit structure, which is characterized by a current fed or voltage fed on one side. The buck type is to have energy storage placed on the high voltage side, and the boost type is to have it placed on the low voltage side. To realize the double sided power flow in bidirectional dc-dc converters, the switch cell should carry the current on both directions. Unidirectional semiconductor power switches such as power MOSFET or IGBT in parallel with a diode [2], [10], because the double sided current flow power switch is not available. For the buck and boost dc-dc type converters, the bidirectional power flow is realized.

- R.Karthikeyan is currently pursuing masters degree program in power electronics & drives engineering in Anna University, Regional centre Coimbatore, India, PH-9566508184. E-mail: karthi4eie@gmail.com.
- A.Santhosh Kumar & D.Deenadayalan is currently pursuing masters degree program in power electronics & drives engineering in Anna University, Regional centre Coimbatore, India, PH-8122582667 & 9941555066. E-mail: newsanthosh@mail.com, ddayalan.eee@gmail.com.

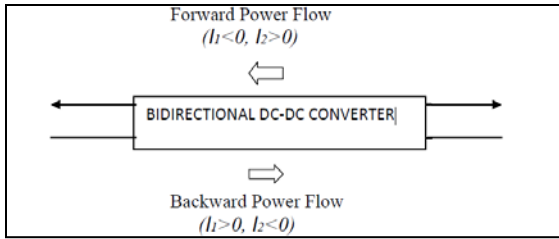


Fig. 1- Bi-directional dc-dc converters

### 2.1 Isolated Bidirectional Dc-Dc Converter

In the bidirectional dc-dc converters, isolation is normally provided by a transformer. The added transformer implies additional cost and losses. However, since transformer can isolate the two voltage sources and provide the impedance matching between them, it is an alternative in those kinds of applications [16]. As a current source, inductance is normally needed in between. For the isolated bidirectional dc-dc converters, sub-topology can be a full-bridge, a half-bridge, a push-pull circuit, or their variations the block diagram of FC and SC with two converters is shown in fig 2.

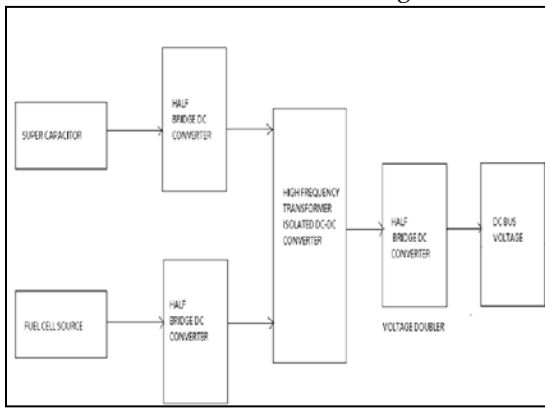


Fig. 2- Block diagram of FCs and SCs individual dc converter.

This converter is well suited for battery charging and discharging circuits in dc uninterruptible power supply (UPS). Advantages of this proposed converter topology include galvanic isolation between the two dc sources using a single transformer, low parts count with the use of same power components for power flow in either direction. The half-bridge based topologies have been developed so far to reduce the device count and increase efficiency. However a voltage imbalance exists between the two split capacitors, thus an additional control circuit to eliminate the voltage imbalance problem is required. The full-bridge bidirectional dc-dc converter is considered one of the best choices. However, this system has a complicated configuration, high cost and large size.

### 2.3 Drawbacks of Two Individual Dc Converter

The Connecting FCs and SCs by two individual dc-dc converters separately to a mutual dc voltage bus is the most

common configuration. It offers many advantages, especially, faster and more stable system response. However, it increases the system cost and power losses. A multiple dc voltage bus, which connects FCs and SCs to different cascaded voltage buses through converters, is also a widely used configuration, but the disadvantages are high power losses and low reliability. Moreover, FCs and the SCs cannot keep the bus voltage constant except if they are oversized.

### 2.2 Full Bridge Converter Method Fc & Sc With Dc Converter

Connected full bridge converter dc converter the simplest configuration is to parallel FCs and SCs directly as shown in fig 3. With one power source but their output currents cannot be controlled independently. In addition, a multiport configuration was introduced. A multiport current-fed dc-dc converter based on the flux additivity was proposed in. To overcome this drawback, two current-fed dual-input bidirectional converters were proposed and investigated.

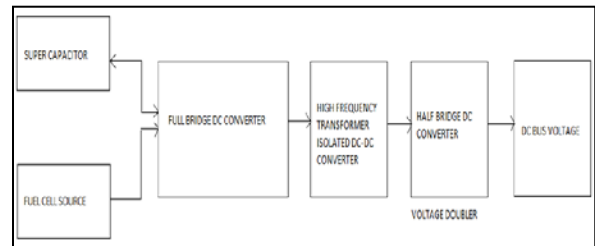


Fig. 3- Block diagram of FCs and SCs

The solutions based on the dual-active-bridge converter using magnetic coupling transformer were presented in, where the bidirectional power can be regulated by phase-shift control scheme [11]. Converters using resonant tank or interleaved transformer windings were reported in, respectively. However, the control strategy for the multiport type is not easy to implement.

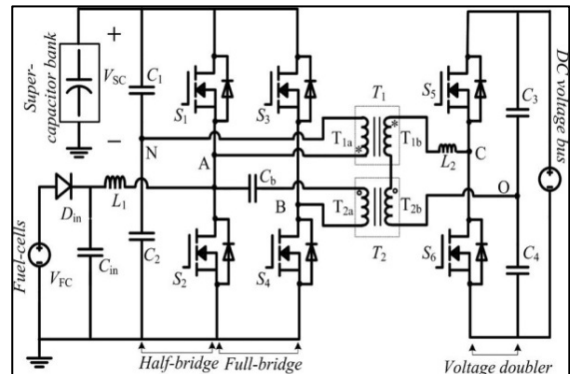


Fig.4. Hybrid bidirectional dc-dc converter topology

As shown in Fig.4, a BHB structure locates on the primary side of the transformer T<sub>1</sub> and it associates with the switches S<sub>1</sub> and S<sub>2</sub> that are operated at 50% duty cycle. The SC bank as an auxiliary energy source is connected to the variable low-voltage (LV) dc bus across the dividing capacitors, C<sub>1</sub> and C<sub>2</sub>. Bidirectional operation can be realized between the SC bank and the high-voltage (HV) dc bus. Switches S<sub>3</sub> and S<sub>4</sub> are controlled by the duty cycle to reduce the current stress and ac RMS value when input voltage V<sub>FC</sub> or VSC are variable over a wide range. The transformers T<sub>1</sub> and T<sub>2</sub> with independent primary windings as well as series-connected secondary windings are employed to realize galvanic isolation and boost a low input voltage to the HV dc bus. According to the direction of power flow, the proposed converter has three operation modes that can be defined as boost mode, SC power mode, and SC recharge mode. In the boost mode, the power is delivered from the FCs and SCs to the dc voltage bus. In the SC power mode, only the SCs are connected to provide the required load power.

**i. Boost Mode**

In the boost mode, the timing diagram and typical waveforms are shown in Fig.5, where n<sub>1</sub> and n<sub>2</sub> are the turn ratios of the transformers. The current flowing in each power switch on the primary side is presented, but the voltage and current resonant slopes during the switching transitions are not shown here for simplicity.

To analyze the operation principles clearly, the following assumptions are given: 1) all the switches are ideal with antiparallel body diodes and parasitic capacitors; 2) the inductance L<sub>1</sub> is large enough to be treated as a current source; 3) the output voltage is controlled well as a constant.

**Stage 1 (t<sub>0</sub> –t<sub>1</sub>):**

It can be seen that at any time, the volt-age across L<sub>2</sub> is always V<sub>T1b</sub> + V<sub>T2b</sub> - V<sub>CO</sub>, but V<sub>T1b</sub>, V<sub>T2b</sub>, and V<sub>CO</sub> have different values in different operating intervals. In (t<sub>0</sub> –t<sub>1</sub>), S<sub>1</sub>, S<sub>4</sub>, and S<sub>6</sub> are gated, so V<sub>T1b</sub> = n<sub>1</sub> V<sub>FC</sub>, V<sub>T2b</sub> = 2n<sub>2</sub> V<sub>FC</sub>, and V<sub>CO</sub> = - V<sub>o</sub> /2, and thereby i<sub>L2</sub> will increase linearly. Because i<sub>T1a</sub> + i<sub>T2a</sub> are negative and i<sub>L1</sub> is positive, the current flows through D<sub>S1</sub>, the body diode of switch S<sub>1</sub>. The current paths during this interval are shown in Fig.6 (a).

**Stage 2 (t<sub>1</sub> –t<sub>2</sub>):**

From t<sub>1</sub>, the value of i<sub>T1a</sub> + i<sub>T2a</sub> starts to be positive, and thus S<sub>4</sub> conducts to carry the current, but S<sub>1</sub> may conduct until the value of i<sub>L</sub>.

**Stage 3 (t<sub>2</sub> –t<sub>3</sub>):**

At t<sub>2</sub>, S<sub>6</sub> is turned OFF. The inductor L<sub>2</sub> begins to resonate with the stray capacitors C<sub>S5</sub> and C<sub>S6</sub>. When the voltage across C<sub>S5</sub> reduces to zero, the body diode of S<sub>5</sub> starts to conduct, so the voltage V<sub>CO</sub> equals V<sub>o</sub> /2.

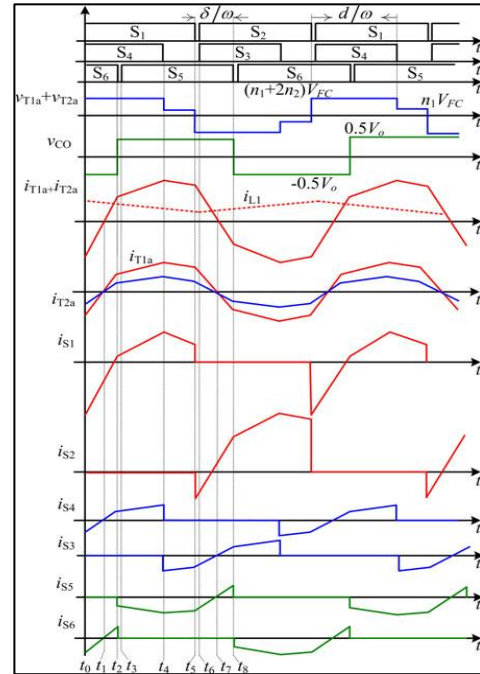


Fig.5. Timing diagram and typical waveforms in the boost mode

**Stage 4 (t<sub>5</sub> –t<sub>6</sub>):**

At t<sub>5</sub>, S<sub>1</sub> is turned OFF. The inductor L<sub>2</sub> begins to resonate with the stray capacitors of the switches.

**Stage 5 (t<sub>4</sub> –t<sub>5</sub>):**

At t<sub>4</sub>, S<sub>4</sub> is turned OFF. The inductor L<sub>2</sub> begins to resonate with the stray capacitors C<sub>S3</sub> and C<sub>S4</sub>. When the voltage across S<sub>3</sub> reduces to zero, D<sub>S3</sub> is, therefore, forward biased. The voltage across the primary winding of T<sub>2</sub> is clamped to zero, i.e., V<sub>T2b</sub> = 0. Hence, V<sub>L2</sub> equals V<sub>T1b</sub> - V<sub>CO</sub> and the current paths are shown in Fig. 6(d).

**Stage 6 (t<sub>5</sub> –t<sub>6</sub>):**

At t<sub>5</sub>, S<sub>1</sub> is turned OFF. The inductor L<sub>2</sub> begins to resonate with the stray capacitors of the switches, C<sub>S1</sub> and C<sub>S2</sub>. C<sub>S1</sub> is charged from approximately 0 V, while C<sub>S2</sub> is discharged from 2V<sub>FC</sub>. The rate of change on voltage depends on the magnitude i<sub>T1a</sub> + i<sub>T2a</sub> - i<sub>L</sub>.

**Stage 7 (t<sub>6</sub> –t<sub>7</sub>):**

During this interval, V<sub>T1b</sub> = - n<sub>1</sub> V<sub>FC</sub>, V<sub>T2b</sub> = - 2n<sub>2</sub> V<sub>FC</sub>, and V<sub>CO</sub> = V<sub>o</sub> /2, so the primary current decays. Until i<sub>L1</sub> is bigger than i<sub>T1a</sub> + i<sub>T2a</sub>, the current starts to flow through the switch S<sub>2</sub>.

**Stage 8 (t<sub>7</sub> –t<sub>8</sub>):**

From t<sub>7</sub>, both i<sub>T1a</sub> and i<sub>T2a</sub> are to be negative, which makes S<sub>3</sub> and S<sub>5</sub> conduct. The equivalent circuit is shown in Fig. 6(f). After t<sub>8</sub>, the second half cycle starts.

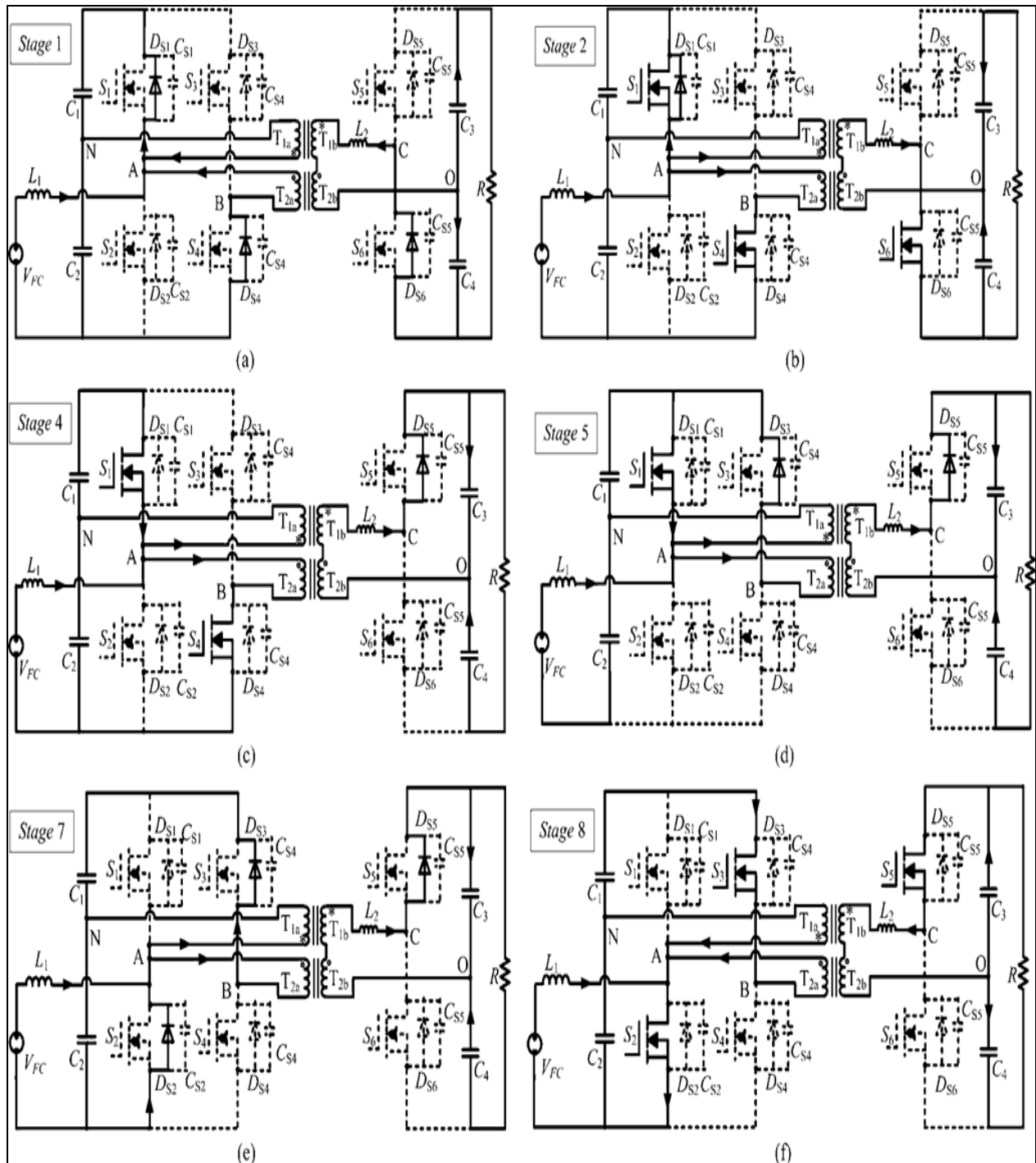


Fig.6 Equivalent circuits in each operating stage: (a) Stage 1, (b) Stage 2, (c) Stage 4, (d) Stage 5, (e) Stage 7, and (f) Stage 8

**ii. SC Power Mode**

For a short period of utility power failure in UPS system that can be handled by SCs or during the fuel-cell warming-up stage, the converter will be operated under the SC power mode and the power flows from SC bank to the dc voltage bus as shown in Fig.7 It can be seen that the typical waveforms are similar with those in the boost mode, but because there is no  $I_{L1}$ , the current stresses of  $S_1$  and  $S_2$  are completely the same.

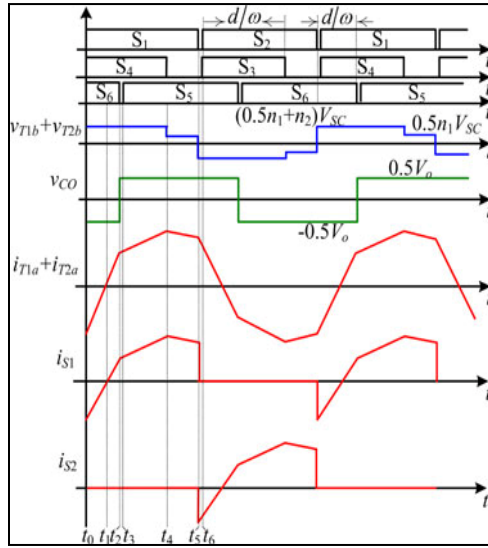


Fig.7. Timing diagram and typical waveforms under the SC power mode.

**iii. SC Recharge Mode**

In the SC recharge mode, the SC will be charged by the HV dc bus which means that the power flows from the HV side to the LV side. The timing diagram and typical waveforms are illustrated in Fig. 8, where the gate drive signal of  $S_5$  is leading to that of  $S_1$  due to the reversed power-flow direction.

**3 Quasi-Optimal Design Method**

To increase the conversion efficiency, generally based on the precise mathematic model of the power loss of each component and the converter switching times, the phase-shift angle, and the duty cycle can be calculated to control the converter and make the total power losses minimal[12],[15]. But this method has two critical limitations in practice 1) performance will suffer when the loss models employed in the circuit and the switching times are not available or not precise; and 2) the controller with the needed phase-shift angle and duty cycle depending on the variable input voltage and output power is complex to design.

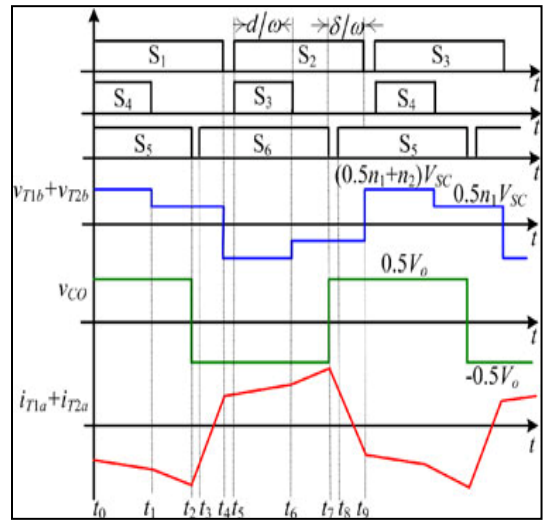


Fig.8. Timing diagram and typical waveforms under the SC recharge mode.

**4 Simulation Results**

A quasi-optimal design is proposed here which includes two design criteria.

- 1) Minimize the RMS value of  $i_{L2}$  by the phase-shift and duty-cycle control to reduce the conduction losses.
- 2) Keep the ZVS operation for HV-side switches to reduce the switching losses.

The RMS current flowing through the secondary inductor is calculated. According to phase-shift angles and duty cycles under the condition where the output power is 1 kW;

The output voltage is 400 V; the interface inductance is 40  $\mu$ H, and the switching frequency is 100 kHz. When the input voltage or the duty cycle varies, the phase-shift angle may be recalculated by (1) to get the required output power or dc-bus voltage. The simulink result of output voltage is presented here. The maximum output voltage is obtained 400V. It can be seen that by adjusting the duty cycle value can reduce the current RMS value effectively. Furthermore, using duty-cycle control can extend the soft-switching range for the HV-side switches,  $S_5$  and  $S_6$ .

The fuel input voltage is given to the boost converter, where it's stepped up voltage is fed to the coupled transformer and one more half bridge is connected in series with dc load to obtain 600-V. The maximum output voltage is obtained by reducing losses and ripples. The proposed converter shows better efficiency for the whole load range compared to the conventional one. It can be used for high power applications.

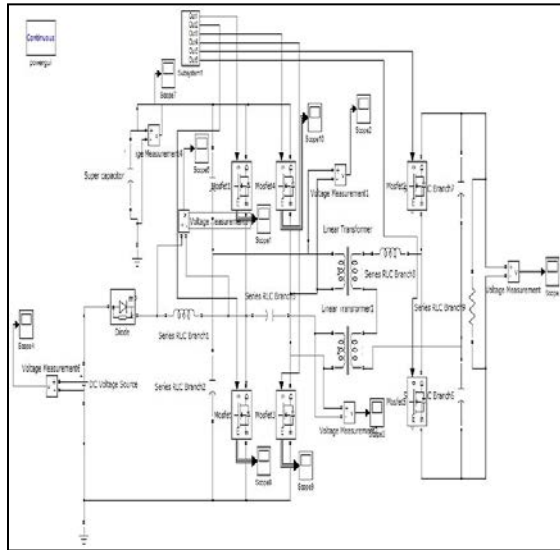


Fig 9 Simulation model of Existing method

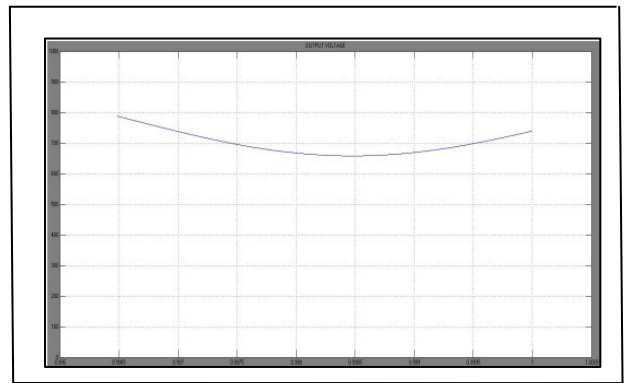


Fig 12. Simulink waveform for output voltage

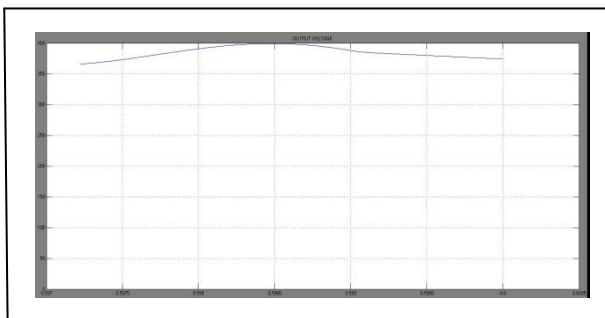


Fig 10. simulink wave form for output voltage

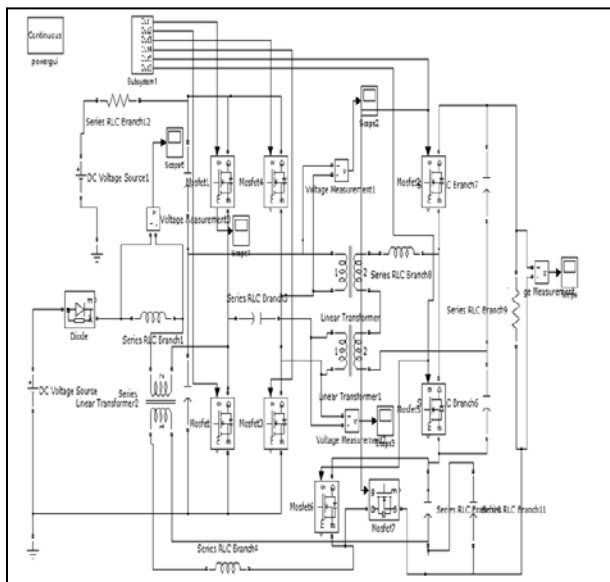


Fig 11 .Simulation model of proposed method

## 5 Conclusion

A novel hybrid bidirectional dc– dc converter consisting of a current-fed input port and a voltage-fed input port was proposed and studied. Using the steady-state analysis, the relationship between the voltage gains of the proposed converter was presented to analyze the power flows. The simple quasi-optimal design method was investigated to reduce the current ac RMS current and extend the ZVS range. Experiments showed good agreement with the theoretical analysis and calculation. Additionally, the experimental results reveal that the duty-cycle control can effectively eliminate the reactive power and increase the efficiency when input voltage is varied over a wide range. So, we can conclude that the proposed converter is a promising candidate circuit for the FC and SC applications. This done by using of MATLAB/SIMULINK. Therefore, this bi-directional isolated dc-dc converter is suitable for high-voltage and high-power applications.

## REFERENCES

- [1]. A. Payman, S. Pierfederici, and F. Meibody-Tabar, "Energy management in a fuel cell/supercapacitor multisource/multiload electrical hybrid system," *IEEE Trans. Power Electron.*, vol. 24, no. 12, pp. 2681–2691, Dec. 2009.
- [2]. W. Liu, J. Chen, T. Liang, R. Lin, and C. Liu, "Analysis, design, and control of bidirectional cascaded configuration for a fuel cell hybrid power system," *IEEE Trans. Power Electron.*, vol. 25, no. 6, pp. 1565–1575, Jun. 2010.

- [3]. J. Bauman and M. Kazerani, "A comparative study of fuel-cell battery, fuel-cell- Ultracapacitor, and fuel-cell-battery-ultracapacitor vehicles," *IEEE Trans. Veh. Technol.*, vol. 57, no. 2, pp. 760–769, Mar. 2008.
- [4]. J. M. Guerrero, "Uninterruptible power supply systems provide protection," *IEEE Ind. Electron. Mag.*, vol. 1, no. 1, pp. 28–38, Spring 2007.
- [5]. K. Jin, X. Ruan, M. Yang, and M. Xu, "Power management for fuel-cell power system cold start," *IEEE Trans. Power Electron.*, vol. 24, no. 10, pp. 2391–2395, Oct. 2009.
- [6]. T. Funaki, "Evaluating energy storage efficiency by modeling the voltage and temperature dependency in EDLC Electrical Characteristics," *IEEE Trans. Power Electron.*, vol. 25, no. 5, pp. 1231–1239, May 2010.
- [7]. H. Matsumoto, "Charge characteristics by exciting-axis voltage vibration method in boost driver with EDLCs," *IEEE Trans. Power Electron.*, vol. 25, no. 8, pp. 1998–2009, Aug. 2010.
- [8]. D.D.-C. Lu and V.G. Agelidis, "Photovoltaic-battery-powered DC bus system for common portable electronic devices," *IEEE Trans. Power Electron.*, vol. 24, no. 3, pp. 849–855, Mar. 2009.
- [9]. J. Shen, K. Rigbers, and R.W. De Doncker, "A novel phase-interleaving algorithm for multiterminal systems," *IEEE Trans. Power Electron.*, vol. 25, no. 3, pp. 741–750, Mar. 2010.
- [10]. Z. Zhang, O. C. Thomsen, and M. A. E. Andersen, "A two-stage dc-dc converter for the fuel cell-supercapacitor hybrid system," in *Proc. IEEE Energy Convers. Congr. Expo.* Sep. 2009, pp. 1425–1431.
- [11]. Z. Qian, O. Abdel-Rahman, and I. Batarseh, "An integrated four-port DC/DC converter for renewable energy applications," *IEEE Trans. Power Electron.*, vol. 25, no. 7, pp. 1877–1887, Jul. 2010.
- [12]. D. Xu, C. Zhao, and H. Fan, "A PWM plus phase-shift control bidirectional DC-DC converter," *IEEE Trans. Power Electron.*, vol. 19, no. 3, pp. 666–675, May 2004.
- [13]. G. G. Oggier, G. O. Garcia, and A. R. Oliva, "Switching control strategy to minimize dual active bridge converter losses," *IEEE Trans. Power Electron.*, vol. 24, no. 7, pp. 1826–1838, Jul. 2009.
- [14]. P. L. Dowell, "Effects of eddy currents in transformer windings," *Proc. IEE*, vol. 113, no. 8, pp. 1387–1394, Aug. 1966.
- [15]. R. Ayyanar and N. Mohan, "Novel soft-switching DC-DC converter with full ZVS—Range and reduced filter requirement—Part I: Regulated output applications," *IEEE Trans. Power Electron.*, vol. 16, no. 2, pp. 184–192, Mar. 2001.
- [16]. Z. Zhang, O. C. Thomsen, and M. A. E. Andersen, "A novel dual-input isolated current-fed DC/DC converter for renewable energy system," in *Proc. IEEE 26th Appl. Power Electron. Conf. Expo.*, Mar. 2011, pp. 1494–1501.